WEP
Warwick Evans Publishing

Transactions on Environment, Energy and Earth Sciences
ISSN: 2960-1924, eISSN: 2960-2300 | Volume 2
ERET 2024

Research on Inflatable Fire Isolation Belt Based on Multi steady State Compression Torsion Composite Energy Absorbing Structure

Shengwen Fu [1], Zhongyu Sun [1, *], Guohui Ren [2], Hao Xu [1], Rongyu Li [1], Shengchang Shang [1]

[1] Ulsan Ship and Ocean College, Ludong University, Yantai City, China, 264025

[2] School of Information and Electrical Engineering, Ludong University, Yantai City, China, 264025

* Corresponding Author Email: sunzy1984@126.com

Abstract. Reducing complications and preventing forest fires is the core of forest fire management When a forest fire occurs, it is of great significance to control forest fires by reason of setting up fire isolation zones In this paper, an unstable firehouse isolation belt based on multiple pressure force composite energy absorbing structure is proposed, and the high heat resistance, high performance and capability of the scheme are verified by simulation experiments The airport part of the fire isolation belt options a dot matrix energy absorbing structure molded by base fiber and resin pre, which uses the pressure difference generated by the temperature difference for rapid impact, and the box uses the hole design to realize the flexible storage of the airport, and crosses and fixes the main part through a new type of ground nail and aramid drop e to divide the forest into small blocks, and can separate the fire area without breaking the ring trees The overall operation is simple, the device is flexible and portable, and can be reused, compared with the traditional fire isolation belt, this device greatly improves the fire prevention efficiency and reduces the fire loss.

Keywords: Finite Element Simulation Analysis, Pre-Impregnated Material Molding, Basalt Fiber, Reverse Check Valve.

1. Introduction

Nowadays, frequent forest fires have caused irreversible impacts on forest ecosystems. The existing forest fire prevention measures mainly include laying fire isolation belts, spraying flame retardants, and other methods. Some scholars have innovated it with the help of traditional forest firefighting methods today. Wang Yarong et al. elaborated on the usage methods and precautions of forest fire isolation belts in different application scenarios [1], and explained the feasibility of their methods; Bao Taozhi et al[2]. invented a new type of concrete fire isolation belt, which uses the water collected from the device in daily life to extinguish fires; Wang Haihui et al. [3] innovated traditional fire isolation belts by constructing suitable isolation belts according to local conditions in different regions, reducing the amount of vegetation removal. However, it is necessary to open up a soil belt before constructing the isolation belt and then plant evergreen broad-leaved trees densely, increasing the cost of construction and maintenance.

However, the above methods for solving forest fire extinguishing have too limited application scenarios, low timeliness and efficiency of fire prevention and extinguishing, consume a lot of manpower, material resources and financial resources, and cause irreversible damage to the forest ecosystem. Therefore, in response to the above issues, a new forest fire prevention model design is proposed in the article, and its feasibility is verified through modeling and simulation using ANSYS. In order to obtain a design scheme for lightweight and high-strength composite material devices under complex forest conditions, a user material subroutine (UMAT) was written in FORTRAN language using finite element simulation software ANSYS based on the equivalent stress criterion. A strength simulation model of an inflatable fireproof isolation belt based on a multi steady state compression torsion composite energy absorbing structure was established under seven levels of strong wind (120.8~182.8 pa) pressure and a 15 ° slope.

By inflating the equivalent pressure difference of the device, designing the reinforcement ribs, designing the appearance, and using simulation analysis methods from part to the whole, the design scheme of a lightweight and high-strength device was optimized. The equivalent force cloud map and total deformation cloud map indicate that the device can effectively enhance the structural strength and meet the requirements of lightweight design and strength in fire environments when designed with composite material energy absorbing structure reinforcement ribs and pressure difference automatic inflation.

2. Design principle and simulation experiment of inflatable fire isolation belt

This design scheme adopts a 410 stainless steel box to connect the airbag, with a dot matrix energy absorbing structure inside the airbag and a new type of ground nail and aramid rope laying scheme outside. When not in use, the airbag contracts in a vacuum state inside the lightweight design box, as shown in Figure 1. When in use, the airbag is manually pulled out from both sides of the box and automatically inflated quickly using the pressure difference, as shown in Figure 2. Due to the plasticity of airbags, the bent device can highly adapt to complex terrain environments, reducing forest damage caused by the installation of fire barriers. And it can flexibly avoid tree obstacles when crossing forests, reduce physical damage, and improve transportation efficiency.

Figure 1. Ununfolded state diagram of the device. **Figure 2.** Expanded state diagram of the device.

2.1. Design of the capsule body

This device is made of basalt fiber and resin raw materials [4-5] in the capsule part, combined with pre impregnated molding process [6]. Basalt fiber is a high-performance and environmentally friendly material made by melting and drawing natural basalt rock. It has high mechanical strength and strong resistance to various chemical substances. It can maintain its physical properties even at extreme temperatures, significantly improving the tensile and bending resistance of the capsule, and can adapt to complex forest working conditions. The specific parameters are shown in Table 1:

Table 1. Parameters related to capsule performance.

BF/PP/PP-g-MA	
mass ratio	30/55/15
Tensile modulus/	one hundred and ninety-five point two
Elongation at break/	ten point one
Tensile strength/	twenty-seven point two three
Bending strength/	ninety-five point zero three
Notch impact strength/	nine point five six

In terms of airtightness, this design adopts a reverse check valve, which has a maximum working pressure of 0.5MPa and belongs to a low-pressure single valve. When the inlet gas pressure rises to a certain value, the air pressure overcomes the pre tightening force of the spring to open the one-way valve. As the inlet pressure gradually decreases, the one-way valve remains sealed under the action of the spring force and prevents the reverse flow of gas. Therefore, to ensure that the one-way valve does not change after adjusting the opening pressure, lock it with a locking nut and add a lead seal to prevent loosening. The airbag is in a vacuum state before use, and during the inflation process, full consideration is given to the preheating of the air in front of the flame in the high-temperature environment of the fire site, forming a low-pressure zone, while the air behind the flame forms a high-pressure zone due to thermal expansion. Utilize the pressure gradient of flame propagation to automatically inflate the airbag.

The internal structure of a check valve consists of components such as the valve body, valve cover, valve disc, spring, and sealing gasket. The relevant parameters and three-dimensional model diagram are shown in Figure 3, and the internal dimensions are shown in Table 2 [7]:

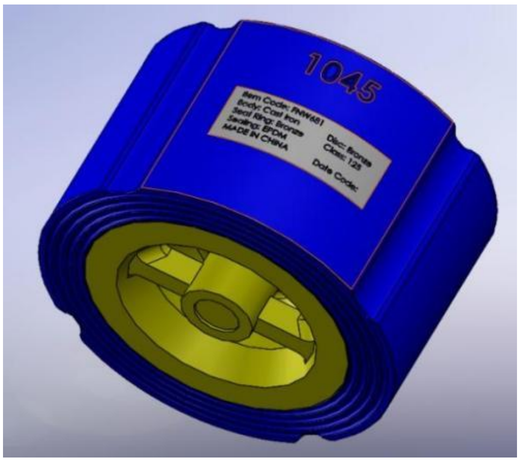

Figure 3. 3D Model of Check Valve.

Table 2. Relevant parameters of check valves.

sample	Outer circle (mm)	Inner hole size and coaxiality/mm		Fit clearance (mm)
		$Ø6^{+0.028}_{+0.01}$	Coaxiality between cone and hole	
one	five point nine six four	6.0.19	zero point zero zero four	zero point zero five five
two	five point nine four six	six point zero two three	zero point zero zero six	zero point zero seven seven
three	five point nine five nine	six point zero two three	zero point zero zero five	zero point zero six seven
four	five point nine five four	six point zero two three	zero point zero zero seven	zero point zero six nine
five	five point nine five five	six point zero two eight	zero point zero zero three	zero point zero seven three

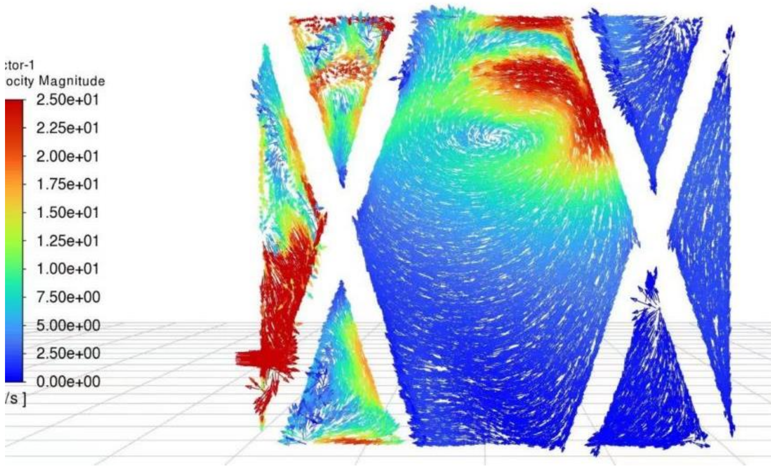

Figure 4. Cloud diagram of capsule inflation.

Under an atmospheric pressure difference of 101325 Pascals (Pa), automatic inflation was carried out using a reverse check valve. ANSYS finite element simulation experiments were conducted, and the results are shown in Figures 4 and 5. The stress at the intake valve is maximum, with a maximum stress of 2.50Pa and a maximum deformation of only 0.376mm. The maximum working pressure of the reverse check valve is 0.5MPa, and the opening pressure does not exceed the indicator requirements. From the stress line graph of the surface path of the capsule, it can be seen that the stress changes are within a reasonable range. Meets material strength and design requirements.

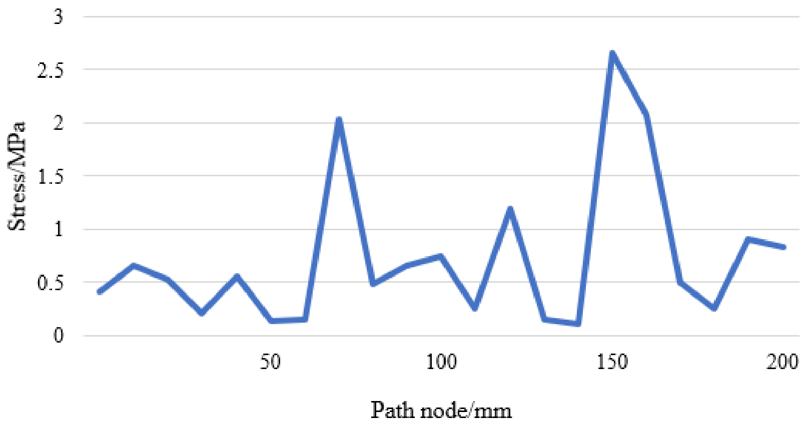

Figure 5. Stress line diagram of the surface path of the capsule body.

2.2. Design of reinforcement ribs

Energy absorbing structures have the advantages of superior impact resistance, strong safety adaptability, and long structural safety life. This device is the first parallel application from the automotive industry to the fire protection industry, with aluminum alloy devices as the research object. Performance equivalent design and optimized forming process are used to comprehensively analyze the performance requirements of components (including strength, stiffness, corrosion resistance, thermal expansion washing, etc.) under the condition of basically unchanged load and environment. Combined with vacuum assisted resin transfer molding (VARTM) process, the interlayer bonding force and overall performance of composite materials are improved. Basalt fiber composite materials have stronger weather resistance and physical properties compared to aluminum alloy materials, so they can be replaced by basalt composite materials.

The energy absorbing structure has a two-dimensional unit array in the plane and parallel stacking outside the plane, with the characteristic of periodic topological division. Compared with the matrix material, it has higher porosity and lower mass density, thus having high specific stiffness, specific strength, and specific energy absorption. The article summarizes and compares the geometric and mechanical characteristics of four topological structures: squares, hexagons, triangles, and circles [8-9], as shown in Figure 6. The use of hierarchical and gradient strategies in macro scale structural design can bring greater flexibility and a wider range of mechanical properties. At the microscopic scale, curved surface transitions and the dispersion and consumption of impact energy guided by holes in stress concentration areas are adopted.

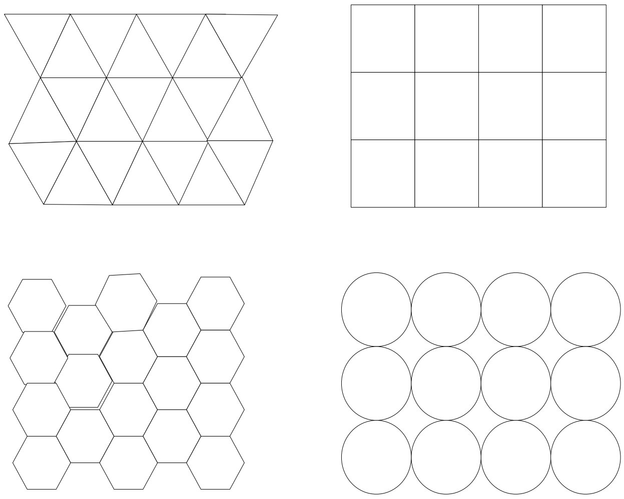

Figure 6. Topological Structure Plan.

2.3. External design of the box and rope laying plan

The box is made of 410 stainless steel, with a length of 540mm, a width of 323mm, and a height of 2000mm. The interior is designed with hollowing out, and the outside of the box is coated with organic silicon high-temperature resistant paint, as shown in Figure 7. The box design scheme can effectively store airbags, with high strength and heat resistance. The lightweight concept can reduce overall weight, and integrated pouring is more convenient for large-scale production.

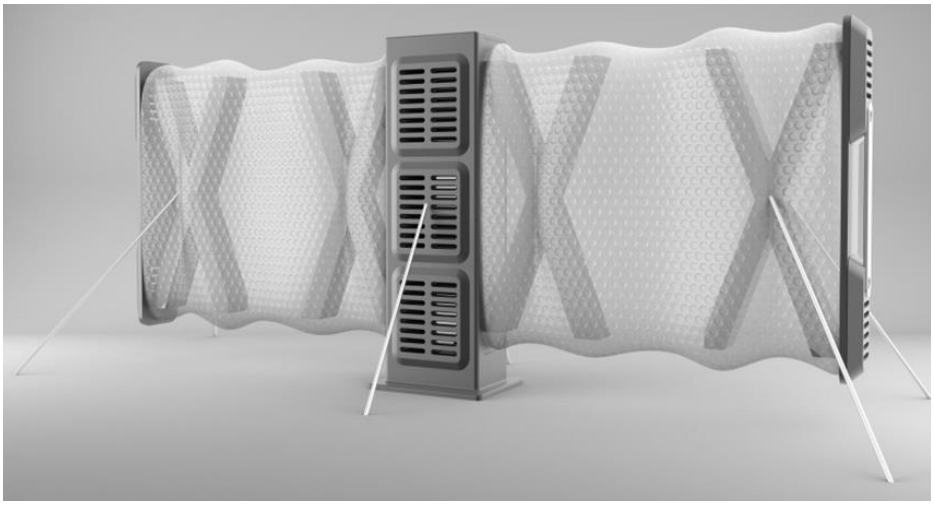

Figure 7. Appearance Design of the Box.

The fixing device of the fire belt adopts the method of aramid rope and ground nails. Ropes are set on both sides of the horizontal axis of each layer of the fire belt, and 4 points are symmetrically set on both sides of the bottom layer. Starting from the third layer, a total of 4 points are symmetrically set on both sides, all set at a distance of 4 meters from the edge. Starting from the fourth layer, 2 points are separately set on the downwind side. For each additional layer, an additional 2 points are set on the upwind and downwind sides, and set at a distance of 4 meters from the lower set points. A total of 16 points are set (including the aramid rope set points). The specific parameters are shown in Table 3. The ground nail is struck at an external angle of 45-60 degrees in the soil, which has extremely strong stability.

Table 3. Fixed Rope Length.

Number of layers	Length/m
W	one
H	six
bottom	zero point five seven seven
Third layer	two point eight eight six
Fourth layer	four point zero four one
Fifth layer	five point one nine six
Sixth layer	six point three five one

3. Overall performance evaluation of the device in this plan

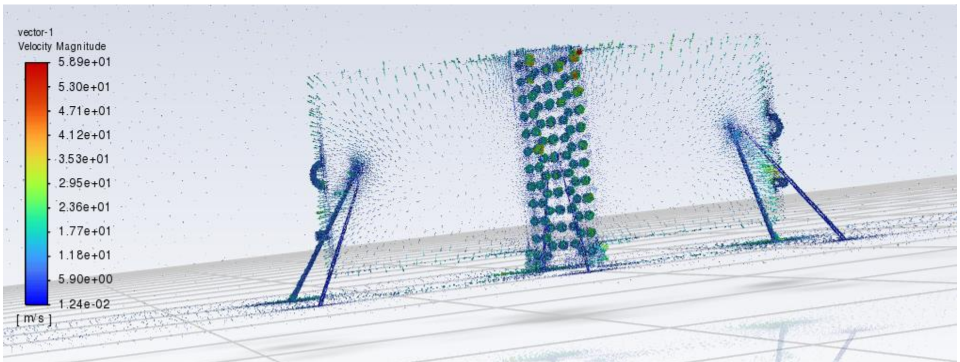

Figure 8. Global Vector Graph.

Based on the physical model grid division and the parameter settings and boundary conditions of turbulent and multiphase flow models under complex operating conditions, a linear solver is used to analyze fluid flow characteristics, predict fluid behavior, and optimize design parameters. The vector diagram is shown in Figure 8, where the arrow direction and arrow length of the visible global vector indicate the diffusion of the global fluid from the center to all directions, with a minimum velocity of 0.01236262m/s and a maximum velocity of 58.90007m/s.

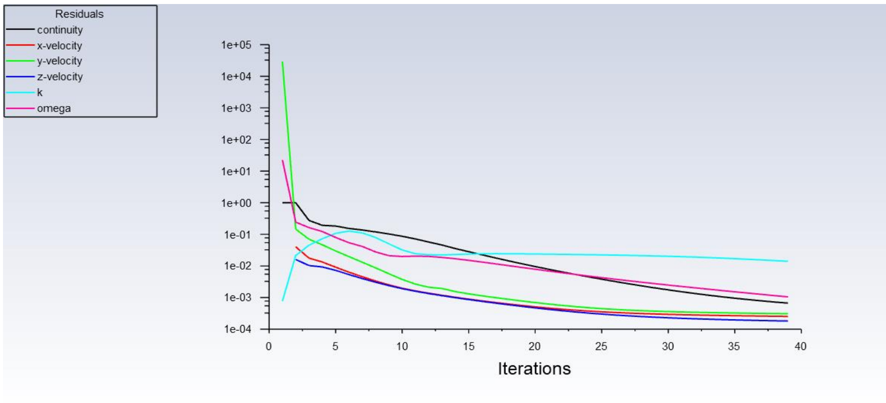

Figure 9. Residual plot.

$$\partial^2 = \frac{(y\{n+1\}-y\{n\})}{y\{n\}} \quad (1)$$

Among them,The residual plot is shown in Figure 9 and the residual formula is shown in (1), where y_ {n+1} is the result of the n+1st iteration, and y_ {n} is the result of the n th iteration. By subtracting the results of two adjacent iterations and calculating their absolute values, and then normalizing them, this paper obtains the global residual. As the number of iterations increases, the residual value decreases and stabilizes within a certain interval, indicating that the numerical solution is closer to the true solution, indicating better convergence of the model.

Taking into full consideration the complex geological environment and external factors, by setting a 7-level wind pressure (with wind speeds ranging from 13.9 to 17.1m/s and wind pressures ranging from 120.8 to 182.8pa) and 15 degree slope angle external environmental conditions, a combination of static and transient structural analysis methods is used to not only consider the behavior of the model under static loads, but also reveal the stress, strain, and displacement analysis of the model under fixed or long-term constant loads. We also considered its response under dynamic loads, fully considering time factors, including changes in load, structural vibrations, and other possible dynamic effects. So as to more accurately evaluate the performance and security of the model.

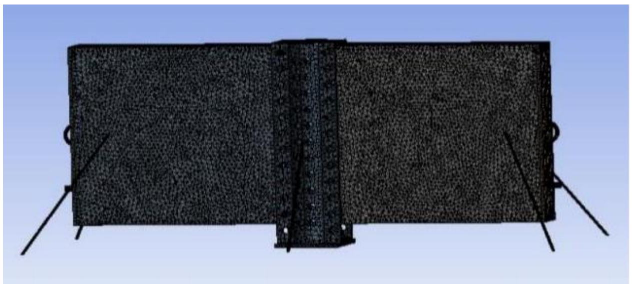

Figure 10. Grid Division Diagram.

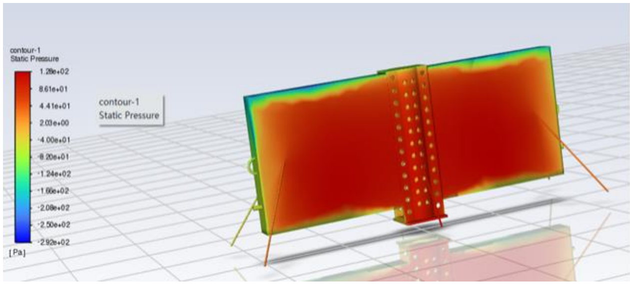

Figure 11. Static structural stress cloud map.

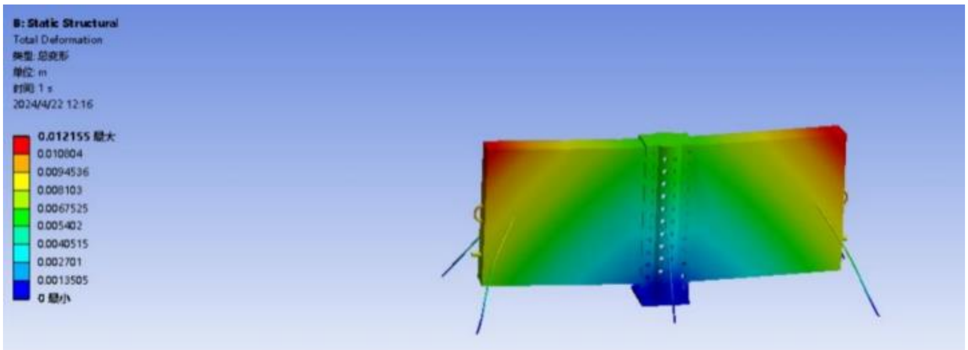

Figure 12. Total deformation diagram of static structure.

When processing the grid, it is necessary to fully consider the structural stress mode and connection mode of the isolation strip. To improve the accuracy of the analysis results, this article adopts automatic grid division on the box and energy absorbing structure, with a unit structure set to 0.001 m. As shown in Figure 10.After partitioning, the number of grid elements is 1233043 and the number of nodes is 4919684. In order to avoid stress concentration and make the simulation results more adaptable to complex structures, manual grid partitioning is used for the connection between airbag corners, ropes, and the ground. Using orthogonal quality evaluation, the average quality of the grid is 0.69956, which meets the requirements. This article only establishes a finite element model and analyzes the stress and deformation of the unfolded state of the fire isolation belt under the set working conditions. This state is also the most dangerous state, and the states of other isolation belts will not be repeated. As shown in Figures 11 and 12, the isolation belt generated maximum strain at the corners of the airbags on both sides under static pressure of 120.8 to 182.8 Pa, with a deformation amount of 0.012155 mm and a maximum stress of 126 Pa. However, the maximum deformation position and maximum stress section are not consistent, indicating that the fire isolation belt proposed in this paper can adapt to static pressure loads under complex working conditions.

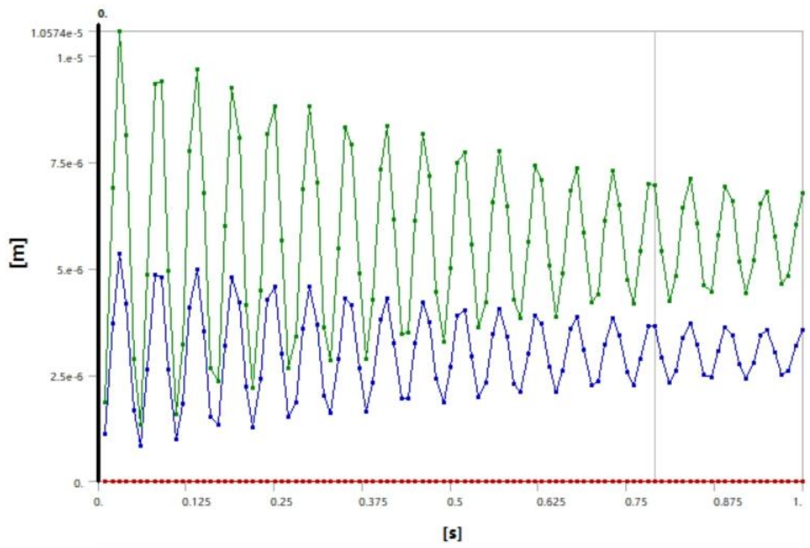

Figure 13. Speed Response Curve.

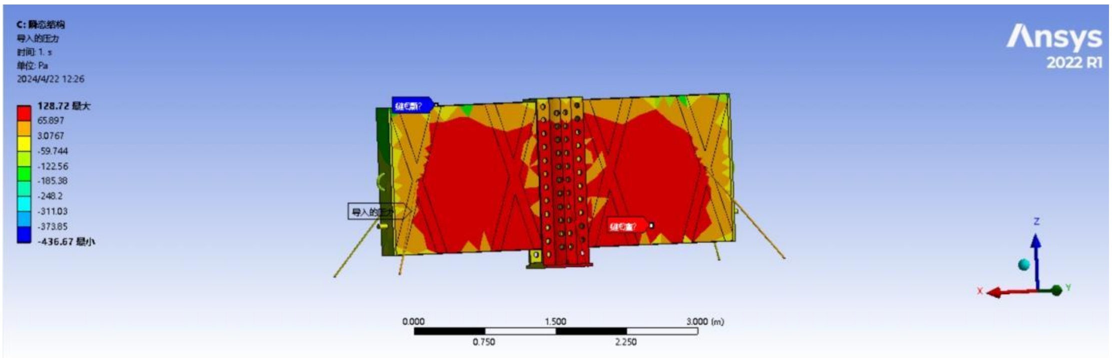

Figure 14. Transient structural stress cloud map.

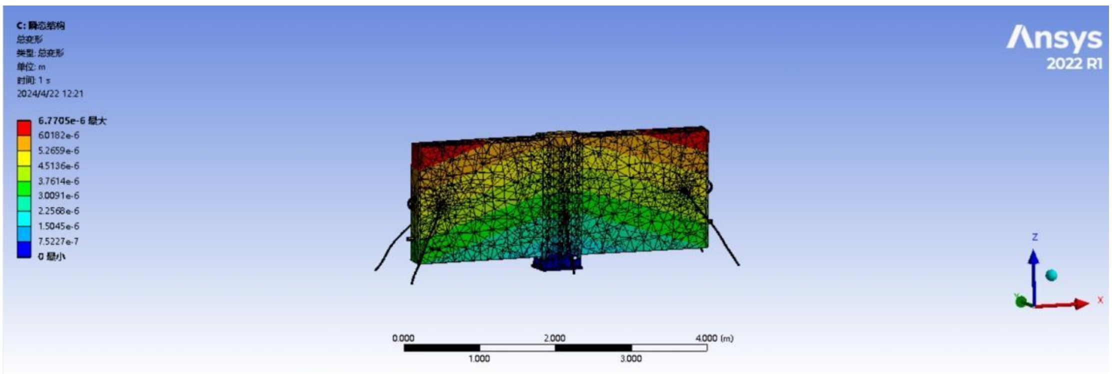

Figure 15. Transient structural stress cloud map.

Taking into full consideration the dynamic loads and transient effects involved in practical engineering problems, this article combines transient structural analysis with static structural analysis to better reflect the behavior characteristics of isolation bands in dynamic processes. As shown in Figures 13, 14, and 15, the maximum stress occurs at the forward section, with a maximum deformation of 0.0000067705 and a maximum stress of 128.72Pa. In transient structural analysis, the velocity response curve suddenly increases at t=0.01s, followed by a gradual easing of the response curve and finally a plateau. The variation of the velocity response curve is consistent with the transient structural modal changes, indicating that the model is sufficient to adapt to the dynamic loads and transient effects of practical engineering problems [10].

4. Conclusion

The interior of the airbag adopts an energy absorbing structure, and the use of a lattice energy absorbing structure can enhance the support and stability of the airbag. The material of the energy absorbing structure is basalt fiber, which has high strength and stiffness as well as good heat resistance, making it suitable for forest firewalls. The box adopts a hollow design, and the lightweight design can reduce the overall weight. Integrated pouring is convenient for large-scale production. The inflation device adopts a reverse check valve, which utilizes the pressure difference generated by temperature difference. Recently, Venus has better performance compared to metal gas cylinders (steel cylinders, aluminum alloy seamless gas cylinders) and greatly reduces the safety hazards brought by metal gas cylinders. This device can quickly inflate while ensuring safety, enabling the establishment of fire belts as soon as possible, quickly preventing the spread of fires, effectively reducing further energy consumption and pollutant emissions, and greatly reducing the time problems caused by existing technologies. The material is made of environmentally friendly materials, and the device can be recycled multiple times, reducing operating costs. The operation is simple, and the number of components is small, which can effectively improve fire extinguishing efficiency.

Compared to most current forest fire isolation zones, trees need to be cut down and large open spaces set up to block combustibles and fires. But this device divides the forest into small pieces to prevent the forest fire from continuing to spread. It can separate the fire area from the outside world without breaking through trees, which is simple and fast, buying valuable time for firefighting.

References

[1] Wang Yarong, Wang Jin, Li Xiaozhong, et al. The Application of Isolation Belt Setting in Forest Fire Extinguishing Practice: A Case Study of Fire Extinguishing in the Central Yunnan Forest Region [J]. Forest Fire Prevention, 2023,41 (01): 35-39

[2] Bao Taozhi, Li Yuping New Forest Fire Isolation Belt [P] Gansu Province: CN202222230787.22022-12-30

[3] Wang Haihui, Tao Junjun, Sheng Changdong. The Transformation and Advantages of Forest Fire Isolation Belt Technology [J]. World Forestry Research, 2015,28 (06): 46-52.

[4] Deng Yibo Preparation and Performance Control of Basalt Fiber Reinforced Composite Materials [D]. Anhui University of Science and Technology, 2023.

[5] Shui Tao, Li Zhen, Xiang Dong, et al. Interface strengthening and mechanical properties of basalt fiber/epoxy resin composite materials [J]. Plastic Industry, 2023,51 (05): 95-101+154

[6] Hou Jiatong Research on the forming process of thermosetting prepreg based on pre pressing and hot-pressing curing [D]. Harbin Institute of Technology, 2024.

[7] Wang Mengli, Zheng Gaofeng, Hou Yun, et al. Design parameters and process optimization of a one-way valve [J]. Hydraulic Pneumatic and Sealing, 2023,43 (09): 97-100

[8] Xu Peng, Xia Dongwei, Wang Chengqiang, et al. Theoretical, numerical simulation, and experimental research on quasi-static compressive stress of reinforced honeycomb [J]. Mechanical Strength, 2024,46 (01): 87-95.

[9] Chang Q, Feng J, Shu Y Advanced honeycomb designs for improving mechanical properties: A review [J] Composition Part B, 2021,227

[10] Fan Dongyang, Li Huazhi, Su Rui, et al. Simulation analysis of construction elevator reducer box based on ANSYS [J]. Journal of Chengdu Institute of Technology, 2018,21 (03): 9-12.